Gamma-rays and neutrinos from RX J1713−3946 in a lepto−hadronic scenario

Pierre Cristofari, Viviana Niro, Stefano Gabici

Monthly Notices of the ROYAL ASTRONOMICAL SOCIETY
MNRAS **508,** 2204–2209 (2021) https://doi.org/10.1093/mnras/stab2380

Gamma-rays and neutrinos from RX J1713–3946 in a lepto–hadronic scenario

P. Cristofari,[1]★ V. Niro[2] and S. Gabici[2]
[1]*LUTH, Observatoire de Paris, 5 place Jules Jansen, F-92195 Meudon, France*
[2]*Université de Paris, CNRS, Astroparticule et Cosmologie, F-75006 Paris, France*

Accepted 2021 August 9. Received 2021 August 9; in original form 2021 May 20

ABSTRACT

The gamma-ray emission of RX J1713–3946, despite being extensively studied in the GeV and TeV domains, remains poorly understood. This is mostly because, in this range, two competing mechanisms can efficiently produce gamma-rays: the inverse Compton scattering of accelerated electrons, and interactions of accelerated protons with the nuclei of the interstellar medium (ISM). In addition to the acceleration of particles from the thermal pool, the re-acceleration of pre-existing cosmic rays is often overlooked, and has in fact also been taken into account. Especially, because of the distance to the SNR ($\sim$1 kpc), and the low density in which the shock is currently expanding ($\sim 10^{-2}$ cm^{-3}), the re-acceleration of cosmic-ray electrons pre-existing in the ISM can account for a significant fraction of the observed gamma-ray emission, and contribute to the shaping of the spectrum in the GeV–TeV range. Remarkably, this emission of leptonic origin is found to be close to the level of the gamma-ray signal in the TeV range, provided that the spectrum of pre-exisiting cosmic-ray electrons is similar to that observed in the local ISM. The overall gamma-ray spectrum of RX J1713–3946 is naturally produced as the sum of leptonic emission from re-accelerated cosmic-ray electrons, and a subdominant hadronic emission from accelerated protons. We also argue that neutrino observations with next-generation detectors might lead to a detection even in the case of a lepto–hadronic origin of the gamma-ray emission.

Key words: stars: general – cosmic rays – gamma-rays: general.

1 INTRODUCTION

Supernova remnants (SNRs) are crucial targets of interest for the gamma-ray community. Indeed, the gamma-ray emission in the GeV and TeV range originating from numerous SNRs clearly demonstrates that efficient particle acceleration is taking place. The detection, so far, of at least 30 SNRs in the GeV range (Ackermann et al. 2015) and 12 SNRs in the TeV range (Abdalla et al. 2018a) also strongly supports the idea that SNRs produce the bulk of Galactic cosmic rays (CRs). This idea is supported by several strong arguments, such as, for example, the fact that SNRs can inject into the ISM particles accelerated through diffusive shock acceleration (DSA) with a spectral distribution compatible with CR measurements at the Earth, and that they can account for the CR energy density at the Earth (see e.g. Drury 2012; Blasi 2013). However, there are several obstacles to this idea (see e.g. Tatischeff & Gabici 2018; Gabici et al. 2019). Let us, for instance, mention two major issues: (i) the fact that all detected SNRs seem not to be able to accelerate PeV particles, which is required for the sources of Galactic CRs; (ii) our inability to clearly understand the mechanisms at stake in the production of gamma-rays in the GeV and TeV range. Indeed, in these energy ranges, two mechanisms can efficiently produce gamma-rays: a hadronic mechanism, which is the production of neutral pions in the interaction of accelerated protons with nuclei of the interstellar medium (ISM) subsequently decaying into gamma-rays; and a leptonic mechanism, which is the inverse Compton scattering of accelerated electrons with soft photons (cosmic microwave background, infrared or optical).

RX J1713–3946 is one of the best studied SNRs in the gamma-ray domain, and perfectly illustrates the difficulties faced when disentangling two possible mechanisms. In the literature, there have been extensive discussions concerning the importance of the leptonic and hadronic mechanisms, or a mixture of the two. Although different scenarios have successfully managed to account for the observed gamma-ray emissions, so far, a consensual and definitive interpretation of the high-energy emission is still missing (Berezhko & Völk 2008; Morlino, Amato & Blasi 2009; Fang et al. 2009; Yamazaki, Kohri & Katagiri 2009; Casanova et al. 2010; Zirakashvili & Aharonian 2010; Ellison et al. 2012; Dermer & Powale 2013; Yang & Liu 2013; Kuznetsova et al. 2019; Tsuji et al. 2019; Zhang & Liu 2019; Fukui et al. 2021).

It is commonly believed that a 'peaked' shape of the gamma-ray spectrum tends to favour a leptonic mechanism (Abdo et al. 2011a; Abdalla et al. 2018b), which naturally produces a compatible shape. However, in the case of RX J1713–3946, a leptonic gamma-ray spectrum would be too narrow if only one population of electrons accelerated at the shock is considered (Finke & Dermer 2012). Moreover, it has been pointed out that a hadronic origin can produce a good fit to the gamma-ray data, for an SNR shock expanding in a clumpy medium (Fukui et al. 2012; Gabici & Aharonian 2014; Celli et al. 2019).

Recently, several authors have indicated that in addition to the acceleration of particles from the thermal bath at a SNR shock, the re-acceleration of already energized particles (i.e. CRs in the ISM) could also lead to a substantial contribution to the total gamma-ray

★ E-mail: pierre.cristofari@obspm.fr

emission. Especially, for SNRs expanding in a low-density ISM ($n \sim 10^{-2}$ cm^{-3}), the ram pressure of the shock ($\propto n v_{\rm sh}^2$) converted into CRs and the target density can be sufficiently low to provide a situation where the gamma-rays from inverse Comption scattering of re-accelerated CR electrons becomes a significant contribution to the total gamma-ray emission (Cristofari & Blasi 2019). Remarkably, such gamma-ray emission relies on only one assumption: the fact that the strong shock expands in a medium with a distribution of CRs that is the one measured at the Earth. It does not depend on the density in which the SNR shock expands, the velocity of shock, or an injection efficiency. The gamma-ray emission from re-accelerated electrons can therefore be seen as a lower limit on the leptonic emission, which exists regardless of any property of the shock.

In this context, we illustrate that the gamma-ray emission of RX J1713–3946 can naturally be accounted for by considering the re-accelerated electrons, and an injection of protons from the thermal pool, straightforwardly producing the observed broad bump in the overall GeV–TeV range. We additionally compute the number of neutrinos expected in the $\gtrsim 1$ TeV range in such a mixed lepto–hadronic scenario. We illustrate that within 10–20 yr of observations with next-generation instruments going beyond the km^3 volume (e.g. Adrián-Martínez et al. 2016a) a detectable neutrino signal can still potentially be expected even in lepto–hadronic scenarios.

The mixed lepto–hadronic scenario presented in this paper is based on the assumption that the spectrum of CR electrons pre-existing upstream of the SNR shock is identical to the one measured in the local ISM. However, as the spatial distribution of CR electrons in the Galaxy is not well constrained, and might be characterized by significant spatial variations at both very large (Atoyan, Aharonian & Völk 1995) and very low (Phan, Morlino & Gabici 2018) particle energies, we conclude that neutrino observations of RX J1713–3946 are mandatory in order to distinguish between different scenarios for the origin of its gamma-ray emission.

2 PRODUCTION OF HIGH-ENERGY PROTONS AND ELECTRONS

2.1 Acceleration of particles from the thermal pool

The acceleration of particles around the strong non-relativistic SNR shock waves (of compression factor $r = 4$) expanding after the explosion of the parent supernova (SN) is assumed to be a result of DSA. It is described with the usual assumption that a fraction ξ of the ram pressure $\rho v_{\rm sh}^2$ is converted into CRs, where $v_{\rm sh}$ is the shock speed. The CR proton spectrum at the shock is $f^{\rm p}(p,t) = A(t)[p/(m_{\rm p}c)]^{-\alpha}$, with $\alpha = 3r/(r-1)$ and the normalization A is $A(t) = (3/4\pi)\xi\rho v_{\rm sh}(t)^2/[m_{\rm p}^4 c^5 I(\alpha)]$, with

$$I(\alpha) = \int_{p_{\rm min}/m_{\rm p}c}^{p_{\rm max}(t)/m_{\rm p}c} {\rm d}x \frac{x^{4-\alpha}}{(1+x^2)^{1/2}}.$$

This spectrum is exponentially suppressed at $p_{\rm max}(t)$.

The spectrum of electrons accelerated from the thermal pool can subsequently be expressed as (Morlino et al. 2009; Zirakashvili & Aharonian 2007)

$$f^{\rm e}(p,t) = K_{\rm ep} f^{\rm p}(p,t) \left\{1 + 0.523 \left[\frac{p}{p^{\rm e}_{\rm max}(t)}\right]^{9/4}\right\}^2 \times \exp\left\{-\left[\frac{p}{p^{\rm e}_{\rm max}(t)}\right]^2\right\}, \quad (1)$$

where $K_{\rm ep}$ is the electron-to-proton ratio, and $p^{\rm e}_{\rm max}$ is the maximum momentum of electrons.

2.2 Re-acceleration of pre-existing CRs

Pioneering works on DSA have already stressed the potential importance of the re-acceleration of pre-existing energized particles in the medium in which the SNR shocks expand (Bell 1978). In the case of an infinite plane shock, the formalism presented in detail in Blasi (2004, 2017) is helpful to understand that the pre-existing CRs can be seen, in a stationary problem, as a boundary condition upstream infinity of the shock for the solution of the transport equation describing particles accelerated at the shock. Such a boundary condition leads to an additional term that describes the particles re-accelerated at the shock, because of the presence of seed particles far upstream of the shock f_∞. In such formalism, the re-acceleration of pre-existing particles obtained, in the absence of non-linear effects, is

$$f_{\rm reac}(p) = \alpha \int_{p_0}^{p} \frac{{\rm d}p'}{p'} \left(\frac{p'}{p}\right)^{\alpha} f_\infty(p'). \quad (2)$$

Remarkably, the expression of the spectrum of re-accelerated particles at the shock depends on very few ingredients: the shock compression factor through the parameter $\alpha = 3r/(r-1)$, the minimum momentum above which re-acceleration occurs p_0, and, of course, the presence of seed CRs f_∞. In the case of a strong shock and in the test particle limit, $\alpha = 3r/(r-1)$ is known and is equal to 4.

As discussed in Blasi (2017), p_0 is of little importance for the shape and normalization if the considered seeds are Galactic CRs, and provided that p_0 is sufficiently low. Indeed, for momenta below $\sim$1 GeV/c, the electron and proton spectra are harder than p^{-4}, so the integral over momentum in equation (2) is dominated by momentum $\sim mc$ at low momenta, and by larger momenta above mc. In the following, we assume that $p_0 = p_{\rm inj} = 10^{-2}\ mc$. In this work, our main assumption is that the seed electrons and protons in which RX J1713–3946 expands are Galactic CRs. We use parametrized descriptions of the unmodulated CR spectra provided for Galactic protons and electrons in Bisschoff, Potgieter & Aslam (2019). These descriptions are in good agreement with data collected by *Voyager* (Cummings et al. 2016) or PAMELA (Adriani et al. 2011a, b), and we introduce a hardening in the proton and electron spectra $\propto p^{0.1}$ and $\propto p^{0.2}$, at 300 GeV for protons and 100 GeV for electrons to fit the AMS–02 data (Aguilar et al. 2015, 2019), as in Cristofari & Blasi (2019). We assume that the presence of the stellar wind bubble does not significantly affect the ambient CR spectrum. This assumption is reasonable because the liftetime of the wind bubble is $\sim$ Myr, for a typical size of a few tens of parsec, and at $\sim$ GeV the typical diffusion length is about a few hundreds of parsec, therefore giving enough time for CRs to populate the cavity.

2.3 Particles accelerated at RX J1713–3946

The particles (protons and electrons) accelerated and re-accelerated at the shock can either be advected downstream of the shock, or manage to escape upstream of the shock into the ISM. In order to escape the SNR accelerator, particles must be sufficiently energized, so that the flux of escaping particles is often described as a delta function peaked around $p_{\rm max}(t)$. In this work, we do not consider this flux of escaping particles, as the gamma-ray emission of the SNR is largely dominated by the flux of the particle advected downstream of the shock, which we consider to be trapped downstream of the expanding shock. From the beginning of the free expansion phase t_0 to a time T, the total number of particles trapped downstream of the

shock is

$$N(p) = \int_{t_0}^{T} \mathrm{d}t \frac{4\pi}{r} r_{\rm sh}^2(t) v_{\rm sh}(t) [f(p) + f_{\rm reac}(p)] \,. \quad (3)$$

In the case of RX J1713–3946, we adopt $t_0 = 1$ yr and $T = 1623$ yr.

2.4 Energy losses

The trapped particles suffer adiabatic losses and synchrotron losses (only relevant for electrons). These losses can be taken into account by writing the conservation of the total number of particles inside the SNR. Following a particle of momentum p' accelerated at a time t and whose momentum is p at T, the total number of particles is

$$N_{\rm loss}(p) = \int_{t_0}^{T} \mathrm{d}t \frac{4\pi}{r} r_{\rm sh}(t)^2 v_{\rm sh}(t) \left(\frac{p'}{p}\right)^2 \times [f(p) + f_{\rm reac}(p)] \frac{\mathrm{d}p'}{\mathrm{d}p}, \quad (4)$$

where the changing of momentum is given by

$$\frac{\mathrm{d}p}{\mathrm{d}t} = -\frac{p}{\mathcal{L}} \frac{\mathrm{d}\mathcal{L}}{\mathrm{d}t} + \frac{4}{3} \sigma_{\rm T} c \left(\frac{p}{m_{\rm e} c}\right)^2 \frac{B_{\rm down}^2}{8\pi}. \quad (5)$$

Here, $\sigma_{\rm T}$ is the Thompson cross-section and $\mathcal{L} = [\rho_{\rm down}(t)/\rho_{\rm down}(t')]^{1/3}$ accounts for the adiabatic expansion between time t and t' (for more details, see e.g. Cristofari, Blasi & Amato 2020; Cristofari, Blasi & Caprioli 2021, and references therein).

2.5 Maximum momentum of accelerated particles

The question of the maximum momentum of the accelerated protons and electrons is essential in this problem, as the corresponding cut-off can shape the gamma-ray spectrum. Most updated results indicate that the maximum momentum of particles is dictated by the growth of magnetic instabilities, and instabilities growing with the fastest growth rate dominate the process. The fastest growing modes are expected to be non-resonant hybrid modes, as discussed in Bell (2004). In this case, the maximum momentum of particles is then set by the saturation of the mechanism, typically reached when the growth corresponds to a few ($\mathcal{N}$) e-folds. If $\gamma_{\rm max}$ is the growth rate at the wavenumber where the growth rate is the highest, the saturation condition is $\int_0^t \mathrm{d}t' \gamma_{\rm max}(t') \sim \mathcal{N}$. The number of e-folds met at saturation $\mathcal{N}$ is still poorly constrained. Indeed, typical values are inferred from numerical studies $\mathcal{N} \approx 5$ (Bell et al. 2013), but arguments in favour of values in the range $\sim$3–9 can be made (for a detailed discussion, see e.g. Schure & Bell 2014). The different values of $\mathcal{N}$ could help explain particle acceleration up to the $\sim$ PeV range, or help us to understand the values of magnetic field energy density at SNRs derived from observations (Völk, Berezhko & Ksenofontov 2005).

Assuming a typical value $\mathcal{N} = 5$, we obtain (Bell et al. 2013)

$$p_{\rm max}(t) \approx \frac{3 r_{\rm sh}(t)}{10} \frac{\xi e \sqrt{4\pi\rho(t)}}{\Lambda} \left[\frac{v_{\rm sh}(t)}{c}\right]^2, \quad (6)$$

where $\Lambda = \ln[p_{\rm max}(t)/mc]$. The corresponding amplified magnetic field is

$$\delta B \approx 2\sqrt{3\pi \frac{v_{\rm sh}}{c} \frac{\xi \rho v_{\rm sh}^2}{\Lambda}}. \quad (7)$$

When the SNR shock enters the low-density bubble, the amplification of the magnetic field through the non-resonant growth of instabilities becomes inefficient. We consider that the magnetic field in the bubble is $\approx 5\,\mu$G. The corresponding maximum energy of protons is then estimated using the Hillas criterion, equating the Bohm-like diffusion coefficient to a fraction $\chi \approx 0.05$–0.1 of the shock radius.

Unlike protons, the maximum energy of electrons is affected by energy losses. These can be taken into account equating the time $\tau_{\rm acc}$ to the minimum of the loss time $\tau_{\rm loss}$ and the age of the system. The acceleration time is estimated as (Drury 1983)

$$\tau_{\rm acc} = \frac{3}{v_1 - v_2} \int_0^p \frac{\mathrm{d}p'}{p'} \left[\frac{D_1(p')}{v_1} + \frac{D_2(p')}{v_2}\right], \quad (8)$$

where indices 1 and 2 refer to the region upstream and downstream of the shock, respectively, v is the fluid velocity, so that $v_1 = v_{\rm sh}$ and $v_2 = v_{\rm sh}/r$, and D is diffusion coefficient assumed to be Bohm-like. As illustrated in Cristofari & Blasi (2019), the assumption of a different energy dependence for the diffusion coefficient could result in a reduced maximum energy for the electrons. Finally, we assume that the maximum energy reached by accelerated and re-accelerated particles is the same.

2.6 Dynamics of the SNR shock

We assume that RX J1713–3946 is the remnant of a massive star that led to the explosion of a core-collapse SN. Therefore, the environment in which the SNR shock expands is structured by the history of the parent massive star: in its main sequence, the stellar wind inflates a low-density bubble in pressure balance with the ISM. When entering the red supergiant (RSG) stage, the low-velocity dense wind forms, of typical velocity $u_{\rm w} = 10^6$ cm s^{-1}, mass-loss rate $\dot{M} = 10^{-5}$ M$_\odot$ yr^{-1} and density $n_{\rm w} = \dot{M}/(4\pi m u_{\rm w} r^2)$ (Weaver et al. 1977). When the SN explosion occurs, the SNR shock thus successively expands through the dense RSG wind and the low-density bubble, and finally reaches the unperturbed ISM. The transition between the dense RSG wind and low-density cavity is set by the pressure equilibrium, and occurs at $r_1 = \sqrt{\dot{M} u_{\rm w}/4\pi k n_{\rm b} T_{\rm b}}$, where k is the Boltzmann constant, and the density and temperature of the hot low-density cavity are $n_{\rm b} = 2 \times 10^{-2}$ cm^{-3} and $T_{\rm b} = 10^6$ K in the case of RX J1713–3946. In such an environment, the dynamical evolution of the SNR shock can be described under the thin-shell approximation (Bisnovatyi-Kogan & Silich 1995; Ptuskin & Zirakashvili 2005).

3 HIGH-ENERGY OBSERVABLE MESSENGERS

The distributions of protons and electrons, accelerated and re-accelerated at RX J1713–3946, are shown in Fig. 1. The proton content (accelerated and re-accelerated) dominates over the electron content (re-accelerated electrons). However, because of the different mechanisms of production of gamma-rays, we show that the gamma-ray signal from re-accelerated electrons (interacting with the photon fields) and from accelerated protons (interacting with the ISM) can be at around the same level.

3.1 Radiations from non–thermal particles

The non-thermal protons and electrons accelerated (and re-accelerated) can produce gamma-rays through two mechanisms: pion production in proton–proton (pp) collisions, and inverse Compton scattering (ICS) of electrons on soft photons. The ICS contribution is estimated considering three Galactic photon fields: the cosmic microwave background, far-infrared dust emission and near-infrared stellar emission. These three components are assumed to be black-bodies of temperatures 2.72, 30 and 3000 K and energy densities of 0.261, 0.5 and 1 eV cm^{-3}.

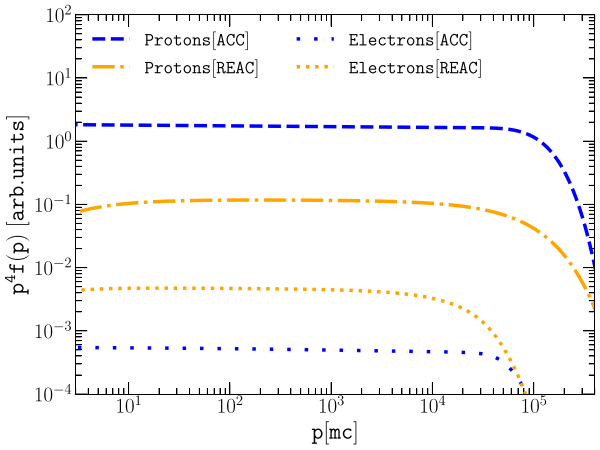

Figure 1. Distribution of particles accelerated at RX J1713–3946. Accelerated protons and electrons are shown by blue dashed and blue dotted lines. Re-accelerated protons and electrons are shown by orange dot-dashed and orange closely dotted lines.

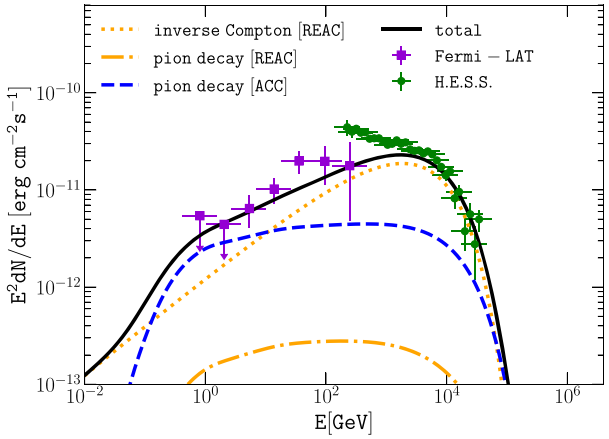

Figure 2. Differential spectrum of RX J1713–3946 obtained with H.E.S.S. (Abdalla et al. 2018b) and *Fermi*/LAT (Abdo et al. 2011b) observations. The dotted (yellow) and dot-dashed (yellow) lines correspond to the gamma-rays from re-accelerated electrons and protons, respectively. The dashed blue line corresponds to freshly accelerated protons. The solid black line is the sum of gamma-rays from freshly accelerated protons and re-accelerated electrons.

The corresponding gamma-rays can be calculated as in Kelner & Aharonian (2008) and Blumenthal & Gould (1970), for instance using the NAIMA package presented in Khangulyan, Aharonian & Kelner (2014). The obtained gamma-ray spectrum is shown in Fig. 2. The total gamma-ray differential flux is also shown (black solid line), and naturally exhibits a large bump, at the level of the *Fermi*/Large Area Telescope (LAT) and High Energy Stereoscopic System (H.E.S.S.) signals. The total emission in the $\sim$ TeV range is dominated by gamma-rays from re-accelerated electrons (dotted yellow line), while the pion decay emission from re-accelerated protons is subdominant (dot-dashed yellow line). However, the GeV part of the spectrum is dominated by the pion decay emission from freshly accelerated protons (assuming an acceleration efficiency of $\sim$10 per cent, compatible with the idea that SNRs are the sources of Galactic CRs). The amount of electrons freshly accelerated at the SNR shock is usually accounted for by introducing an electron-to-

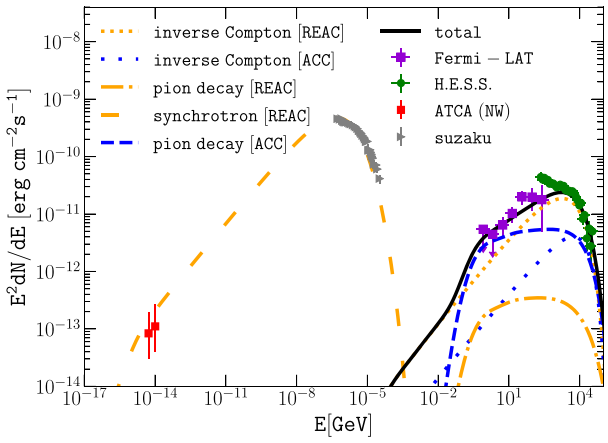

Figure 3. Multiwavelength differential spectrum of RX J1713–3946. Radio and X-ray observations were obtained from the Australia Telescope Compact Array (ACTA; Lazendic et al. 2004) and *Suzaku* (Tanaka et al. 2008). Lines are as in Fig. 2.

proton ratio $K_{\rm ep}$ so that $f^{\rm e}(p) = K_{\rm ep} f^{\rm p}(p)$. Here, $K_{\rm ep}$ is expected to be in the range $10^{-5}-10^{-2}$, but it is not well constrained (Cristofari et al. 2013). In order to explain the gamma-ray emission from freshly accelerated electrons, a typical value of $K_{\rm ep} \approx 10^{-2}$ is needed. In this work, we adopt for illustrative purposes the value $K_{\rm ep} = 10^{-4}$ (Fig. 3), which would lead to a subdominant contribution from freshly accelerated electrons, although higher values of $K_{\rm ep}$ are possible, and would reinforce the signal from re-accelerated electrons.

The synchrotron emission from electrons trapped downstream of the SNR shock is computed in the average magnetic field inside the SNR,

$$\langle B_{\rm down} \rangle = 1/V \int_0^{r_{\rm sh}(T)} {\rm d}r_{\rm sh} 4\pi r_{\rm sh}^2 B_{\rm down}(r_{\rm sh}) \approx 16\,\mu{\rm G},$$

and is found to lead, in the X-ray and radio domains, to a signal at the level of the measured emission. The overall spectrum from the radio to the high-energy gamma-ray domain is shown in Fig. 3.

3.2 Neutrinos

The source is located in the southern sky with a declination of $-38.^{\circ}24$. For this reason, we investigate the possible detection of RX J1713–3946 with the KM3NeT instrument. In this section, we report the calculation for the neutrino events, using the KM3NeT effective area. Following the procedure outlined in Niro et al. (2021), we use the effective area for the detector as reported in Adrian-Martinez et al. (2016b). The event rate is

$$N_{\rm ev} = \epsilon_\nu t \int_{E_\nu^{th}} {\rm d}E_\nu \frac{{\rm d}N_\nu(E_\nu)}{{\rm d}E_\nu} A_\nu^{\rm eff}\,, \qquad (9)$$

where the parameter $\epsilon_\nu = 0.7$ is the visibility of the source. The background of atmospheric neutrinos (Volkova 1980; Gondolo, Ingelman & Thunman 1996; Honda et al. 2011) is then integrated over an opening angle equal to $\Omega = \pi\sigma_{\rm ext}^2$, with $\sigma_{\rm ext} = 0.^{\circ}65$ (see e.g. Aharonian et al. 2006; Abdalla et al. 2018b). The number of neutrino events from the source is calculated considering the expressions given in Kappes et al. (2007); see also Gonzalez-Garcia, Halzen & Niro (2014) and Halzen, Kheirandish & Niro (2017) for a detailed description of the formulae, and Villante & Vissani (2008) for an alternative derivation. Note that the formulae by Kappes et al. (2007) take into account neutrino oscillations, assuming full neutrino

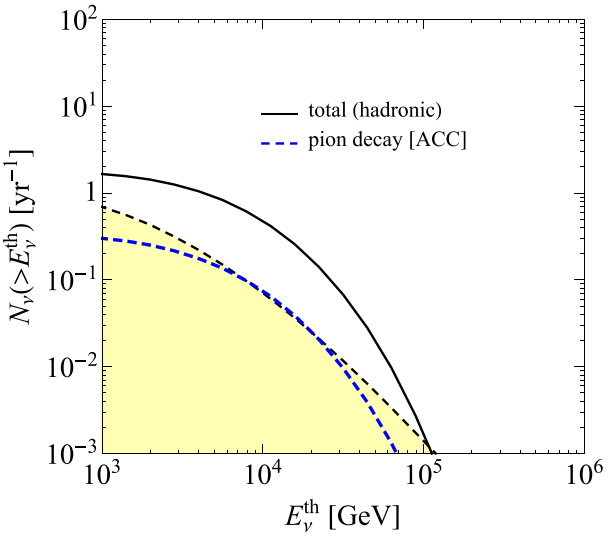

Figure 4. Number of neutrino events at the KM3NeT detector from the RX J1713.7–3946 source compared to the number of events expected by the atmospheric background (yellow shaded area). The black lines refer to the fully hadronic scenario, while blue lines denote the lepto–hadronic case described in this paper (dashed line).

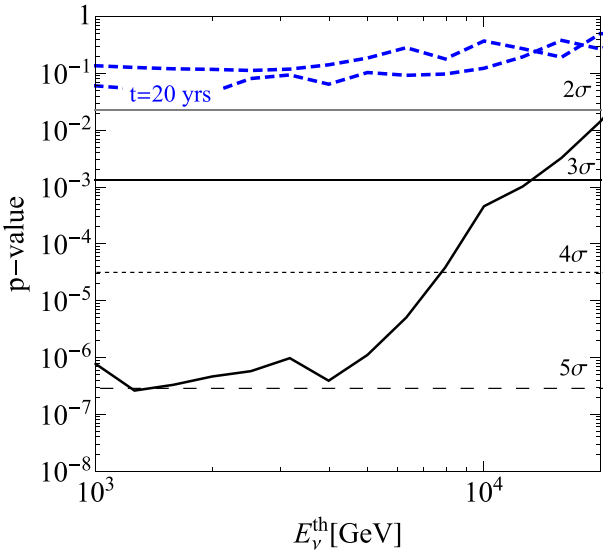

Figure 5. The p-value as a function of neutrino energy threshold for 10 yr of running the KM3NeT detector. Different lines have the same meaning as in Fig. 4. For the case of lepto–hadronic emission, we have also considered 20 yr of running time.

mixing. We find that, assuming that the gamma-rays detected by *Fermi*/LAT and H.E.S.S. are entirely due to hadronic interactions, about ∼1.7 events are expected in 1 yr of observations with KM3NeT and ∼0.7 background events considering an energy threshold of 1 TeV. Our results are in agreement with the results of Costantini & Vissani (2005) and Vissani & Aharonian (2012), if the results reported in these references are rescaled by the visibility (see also Kappes et al. 2007, for a discussion of this topic).

Instead, considering the mixed scenario of leptonic and hadronic emission described above (and illustrated in Fig. 2), about 0.3 events are expected in 1 yr of running the KM3NeT detector for particle energies exceeding 1 TeV. In 10 yr of observations, this would correspond to about three signal neutrinos versus seven background events above 1 TeV.

We report in Fig. 4 the number of events as a function of the neutrino energy threshold for the two scenarios examined above: fully hadronic (solid line) and lepto–hadronic (dashed line). The expected number of background events is also shown as a shaded region. We see from Fig. 4 that in the lepto–hadronic scenario, the number of signal events is of the same order as the background ones for particle energies above ∼10 TeV (of the order of 0.1 neutrinos per year).

In Fig. 5, we show the p-value as a function of the neutrino energy threshold. A 5σ detection can be reached in 10 yr of running the KM3NeT detector for an energy threshold smaller then 5 TeV, if the gamma-ray emission is fully hadronic. Instead, it is difficult to resolve the mixed scenario of leptonic and hadronic emission with a neutrino signal, considering 10 yr of running the KM3NeT detector. Indeed, for this case, the 3σ level is not reached in 10 yr. However, with a higher running time, of about 20 yr, a p-value of the order of several per cent could be reached, corresponding to a hint of an excess of neutrinos (a significance approaching 2σ). Therefore, in this scenario a detection might be well within the reach of extension beyond the km^3 of detectors, as discussed in Adrián-Martínez et al. (2016a).

4 CONCLUSIONS

The numerous discussions on the origin of the gamma-ray emission of RX J1713–3946 illustrate the difficulties in interpreting which is the content in non-thermal accelerated particles. Here we illustrate the importance of taking into account the re-acceleration of pre-existing CR electrons in the case of RX J1713–3946. Remarkably, the amount of re-accelerated particles depends on very few parameters: the density of pre-existing CRs far upstream of the shock, and the minimum momentum above which re-acceleration is efficient. However, the amount of particles accelerated from the thermal pool is typically a fraction of the shock ram pressure $\propto \rho v_{\rm sh}^2$. Therefore, as a remnant of a core-collapse SN, with the shock wave currently propagating in a low-density environment, created during the main sequence of the progenitor star, the situation of RX J1713–3946 provides a case in which the re-acceleration of pre-existing CRs can become comparable to the fresh acceleration of CRs. Let us also note that the re-acceleration of pre-existing CRs does not depend on any CR efficiency.

Moreover, in this low-density environment, the density target material available for proton–proton interaction is reduced, which decreases the amount of gamma-rays from hadronic origin, but does not affect the production of gamma-rays from leptonic origin. This provides us with a situation where the hadronic gamma-ray signal from freshly accelerated protons is at a comparable level to the leptonic gamma-ray signal from leptonic re-accelerated CR electrons.

These two gamma-ray components naturally produce a broad bump in the GeV to TeV range, with a shape compatible with *Fermi*/LAT and H.E.S.S. observations. The overall gamma-ray spectrum is obtained with minimal, physically motivated assumptions. In particular, the slope of accelerated (and re-accelerated) particles is the one expected in the test-particle case $\propto p^{-4}$, and no additional mechanism producing a deviation from $\propto p^{-4}$ at the shock is needed. Also, pre-existing CR protons and electrons around RX J1713–3946 are described by the local unmodulated CR spectrum derived from measurements at the Earth.

Finally, we have calculated the number of neutrinos expected from RXJ1713–3946, and we have estimated the chances of detection with the KM3NeT instrument. In the case of a fully hadronic scenario, the neutrino signal is expected to be a few times above the atmospheric background, making detection in the $\gtrsim 1$ TeV range possible. In the lepto–hadronic scenario presented above, in which the TeV gamma-ray emission is dominating the ICS from re-accelerated electrons, the number of neutrinos expected is reduced and is within the reach of future planned instruments, which are expected to go beyond the km^3 detector volume (Adrian-Martinez et al. 2016b).

The maximum momentum of protons is estimated in the RSG wind from the growth of non-resonant streaming instabilities, as given by equation (6), and when the magnetic field amplification becomes inefficient, using the Hillas criterion. For electrons, the maximum momentum is estimated by equating the acceleration time to the minimum of the synchrotron loss time and the age of the SNR. Alternative hypotheses accounting for a higher level of magnetic field amplification would enhance synchrotron losses, and would make it difficult to explain the gamma-ray spectrum above >10 TeV from the ICS of re-accelerated electrons. Moreover, the recipe used to estimate the maximum energy of electrons relies on the hypothesis that the coefficient diffusion is Bohm-like, although other diffusion models are plausible, but would a priori lead to lower maximum momenta (see e.g. the discussion in Cristofari & Blasi 2019).

The computation of the population of re-accelerated electrons depends on very few ingredients: the fact that the SNR shock is strong, and the presence of CR electrons, considered to be the spectrum measured at the Earth. Let us, however, mention that if the spectrum of CR protons is known to be uniform in the Galactic disc, we do not have solid evidence for CR electrons. Therefore, if important variations were present in the CR electron spectrum in different locations of the Galaxy, our calculation might be substantially affected.

ACKNOWLEDGEMENTS

The authors thank P. Blasi for stimulating discussions and comments. This project has received funding from the European Union's Horizon 2020 research and innovation programme under the Marie Skłodowska-Curie grant agreement No. 843418 (nuHEDGE). SG acknowledges support from Agence Nationale de la Recherche (grant ANR-17-CE31-0014). SG and PC acknowledge support from the Observatory of Paris (Action Fédératrice CTA).

DATA AVAILABILITY

There are no new data associated with this article.

REFERENCES

Abdalla H. et al. 2018a, A&A, 612, A3
Abdalla H. et al., 2018b, A&A., 612, A6
Abdo A. A. et al., 2011a, ApJ, 734, 28
Abdo A. A. et al., 2011b, ApJ, 734, 28
Ackermann M. et al., 2015, ApJ, 807, 169
Adrián-Martínez S. et al., 2016a, J. Phys. G: Nucl. Phys., 43, 084001
Adrian-Martinez S. et al., 2016b, J. Phys. G: Nucl. Phys., 43, 084001
Adriani O. et al., 2011a, Phys. Rev. Lett., 106, 201101
Adriani O. et al., 2011b, Science, 332, 69
Aguilar M. et al., 2015, Phys. Rev. Lett., 114, 171103
Aguilar M. et al., 2019, Phys. Rev. Lett., 122, 101101
Aharonian F. et al., 2006, A&A, 449, 223
Atoyan A. M., Aharonian F. A., Völk H. J., 1995, Phys. Rev. D, 52, 3265
Bell A. R., 1978, MNRAS, 182, 443
Bell A. R., 2004, MNRAS, 353, 550
Bell A. R., Schure K. M., Reville B., Giacinti G., 2013, MNRAS, 431, 415
Berezhko E. G., Völk H. J., 2008, A&A, 492, 695
Bisnovatyi-Kogan G. S., Silich S. A., 1995, Rev. Mod. Phys., 67, 661
Bisschoff D., Potgieter M. S., Aslam O. P. M., 2019, ApJ, 878, 59
Blasi P., 2004, Astropart. Phys., 21, 45
Blasi P., 2013, A&AR, 21, 70
Blasi P., 2017, MNRAS, 471, 1662
Blumenthal G. R., Gould R. J., 1970, Rev. Mod. Phys., 42, 237
Casanova S. et al., 2010, PASJ, 62, 1127
Celli S., Morlino G., Gabici S., Aharonian F. A., 2019, MNRAS, 490, 4317
Costantini M. L., Vissani F., 2005, Astropart. Phys., 23, 477
Cristofari P., Blasi P., 2019, MNRAS, 489, 108
Cristofari P., Gabici S., Casanova S., Terrier R., Parizot E., 2013, MNRAS, 434, 2748
Cristofari P., Blasi P., Amato E., 2020, Astropart. Phys., 123, 102492
Cristofari P., Blasi P., Caprioli D., 2021, A&A, 650, A62
Cummings A. C. et al., 2016, ApJ, 831, 18
Dermer C. D., Powale G., 2013, A&A, 553, A34
Drury L. O., 1983, Rep. Prog. Phys., 46, 973
Drury L. O. C., 2012, Astropart. Phys., 39, 52
Ellison D. C., Slane P., Patnaude D. J., Bykov A. M., 2012, ApJ, 744, 39
Fang J., Zhang L., Zhang J. F., Tang Y. Y., Yu H., 2009, MNRAS, 392, 925
Finke J. D., Dermer C. D., 2012, ApJ, 751, 65
Fukui Y. et al., 2012, ApJ, 746, 82
Fukui Y., Sano H., Yamane Y., Hayakawa T., Inoue T., Tachihara K., Rowell G., Einecke S., 2021, ApJ, 915, 84
Gabici S., Aharonian F. A., 2014, MNRAS, 445, L70
Gabici S., Evoli C., Gaggero D., Lipari P., Mertsch P., Orlando E., Strong A., Vittino A., 2019, Int. J. Mod. Phys. D, 28, 1930022
Gondolo P., Ingelman G., Thunman M., 1996, Astropart. Phys., 5, 309
Gonzalez-Garcia M. C., Halzen F., Niro V., 2014, Astropart. Phys., 57-58, 39
Halzen F., Kheirandish A., Niro V., 2017, Astropart. Phys., 86, 46
Honda M., Kajita T., Kasahara K., Midorikawa S., 2011, Phys. Rev. D, 83, 123001
Kappes A., Hinton J., Stegmann C., Aharonian F. A., 2007, ApJ, 656, 870
Kelner S. R., Aharonian F. A., 2008, Phys. Rev. D, 78, 034013
Khangulyan D., Aharonian F. A., Kelner S. R., 2014, ApJ, 783, 100
Kuznetsova E., Krivonos R., Churazov E., Lyskova N., Lutovinov A., 2019, MNRAS, 489, 1828
Lazendic J. S., Slane P. O., Gaensler B. M., Reynolds S. P., Plucinsky P. P., Hughes J. P., 2004, ApJ, 602, 271
Morlino G., Amato E., Blasi P., 2009, MNRAS, 392, 240
Niro V., Neronov A., Fusco L., Gabici S., Semikoz D., 2021, Phys. Rev. D, 104, 023017
Phan V. H. M., Morlino G., Gabici S., 2018, MNRAS, 480, 5167
Ptuskin V. S., Zirakashvili V. N., 2005, A&A, 429, 755
Schure K. M., Bell A. R., 2014, MNRAS, 437, 2802
Tanaka T. et al., 2008, ApJ, 685, 988
Tatischeff V., Gabici S., 2018, Annu. Rev. Nucl. Part. Sci., 68, 377
Tsuji N., Uchiyama Y., Aharonian F., Berge D., Higurashi R., Krivonos R., Tanaka T., 2019, ApJ, 877, 96
Villante F. L., Vissani F., 2008, Phys. Rev. D, 78, 103007
Vissani F., Aharonian F., 2012, Nucl. Instrum. Meth. A, 692, 5
Völk H. J., Berezhko E. G., Ksenofontov L. T., 2005, A&A, 433, 229
Volkova L. V., 1980, Sov. J. Nucl. Phys., 31, 784
Weaver R., McCray R., Castor J., Shapiro P., Moore R., 1977, ApJ, 218, 377
Yamazaki R., Kohri K., Katagiri H., 2009, A&A, 495, 9
Yang C., Liu S., 2013, ApJ, 773, 138
Zhang X., Liu S., 2019, ApJ, 876, 24
Zirakashvili V. N., Aharonian F., 2007, A&A, 465, 695
Zirakashvili V. N., Aharonian F. A., 2010, ApJ, 708, 965

This paper has been typeset from a TEX/LATEX file prepared by the author.